Original Paper

Effect of AC/DC electrical fields on ZnO nanoparticles kinetics

Marek Kolenčík*[1], Martin Urík[2], Michal Lesňák[3], Karla Čech Barabaszová[3], Marek Bujdoš[2], Martin Šebesta[2], Edmud Dobročka[4], Elena Aydın[5], Eva Duborská[2], Dávid Ernst[1], Martin Juriga[1], Jada Chakvavarthi[6], Yu Qian[7], Huan Feng[8], Gabriela Kratošová[3], B. Ratna Sunil[9], Ramakanth Illa[10]

[1]*Slovak University of Agriculture in Nitra, Faculty of Agrobiology and Food Resources, Institute of Agronomic Sciences, Slovak Republic*
[2]*Comenius University in Bratislava, Faculty of Natural Sciences, Institute of Laboratory Research on Geomaterials, Slovak Republic*
[3]*VŠB Technical University of Ostrava, Nanotechnology Centre, Czech Republic*
[4]*Slovak Academy of Sciences, Institute of Electrical Engineering, Slovak Republic*
[5]*Slovak University of Agriculture in Nitra, Faculty of Horticulture and Landscape Engineering, Institute of Landscape Engineering, Slovak Republic*
[6]*Rajiv Gandhi University of Knowledge Technologies, Department of Electrical and Electronics Engineering, India*
[7]*Yunnan University, School of Ecology and Environmental Science, Yunnan Province, China*
[8]*Montclair State University, Department of Earth and Environmental Studies, NJ, USA*
[9]*Bapatla Engineering College, Department of Mechanical Engineering, India*
[10]*Vellore Institute of Technology – Andhra Pradesh, School of Advanced Sciences, Department of Chemistry, India*

Long-term electrokinetic processes affect the motion of different soil fractions mainly ionic-species in soil-type environments. Primarily, this governs direct (DC) and alternating (AC) electrical fields due to the different thermal, acid-base ion gradients generated close to electrodes resulted in electro-migration, electrophoresis, and other electrolysis-related-processes. The migration of metal ionic-species, including zinc, which occurs mainly under DC electrical field is generally acknowledged, but metal-corresponding nanoforms such as ZnO nanoparticles (ZnO-NP) under low-level DC and AC electrical fields absent in the literature. The aims of the research was the analysis of pressure-driven transport at two different electric potentials; the equipotential-voltage lines in sand-media with ZnO-NP under 1 V, and 3 V (for DC), and AC under 1 V, 3 V (1 kHz of sinusoidal waves), detection of the migration of Zn from ZnO-NP to anode-to-cathode area (DC), and to the electrodes areas for AC with pH changes within three-hours of treatment and X-ray diffraction investigation of structural changes of ZnO-NP. The results showed that the AC electric field had more uniform equipotential-voltage pattern of sand-media than the DC fields for both voltages applied. In addition, different zinc concentrations up to 11% and electro-active substances were detected between the DC anode-to-cathode and Electrode 1 area compared to the AC Electrode 2 area. The higher pH value also correlated only with DC. X-ray diffraction analysis detected no structure transformation of ZnO-NP, but deterioration of relatively stable graphite electrodes appeared. Our results at the low-level AC and DC electrical fields confirmed the potential of electro-accelerated nanoparticle kinetics.

Keywords: effect of AC/DC electrical fields, zinc-oxide nanoparticles, zinc migration, sand medium

1 Introduction

Zinc oxide (ZnO) is an n-type semiconductor with large 3.37 eV band gap energy. It has exceptional optical, electrical, and catalytic properties, which have been demonstrated for the particles of different morphology and size ranges (Kołodziejczak-Radzimska & Jesionowski, 2014). Although the zinc-ionic species are micro-nutrients and were established as an essential component of agrochemicals, at high concentrations they are toxic to

*Corresponding Author: Marek Kolenčík, Slovak University of Agriculture in Nitra, Faculty of Agrobiology and Food Resources, Institute of Agronomic Sciences, Slovak Republic

plants and other biota (Sturiková et al., 2018; Kolenčík et al., 2021).

The ZnO nanoparticles tend to be unstable or dissolve at higher pH under polychromatic light in aqueous solutions (Hamid et al., 2017; Rudd & Breslin, 2000). However, literature provides only limited information on the colloidal stability of ZnO-NP under external electrical fields. It was suggested that ZnO-NP stability depends on the properties of the interface of nanoparticles (NP), which is influenced by:

1. the size, shape and crystallinity of the NP,
2. the electric double layer thickness, structure, and composition,
3. the ambient solution composition, where the NP are spatially dispersed due to repulsive Coulomb-forces (Amde et al., 2017; Kolenčík et al., 2021).

Direct current (DC) and alternating current (AC) electric fields significantly affect the acid-base equilibrium of solutions and accelerate the dissolution of metals, metal oxides and other electro-active substances (Chirakkara et al., 2015). The electric fields accelerate the fluctuation of solution pH (Acar & Alshawabkeh, 1993) causing a gradual change in NP zeta potential, the rate of aggregation, sedimentation, and impaired NP function (Amde et al., 2017; Kolenčík et al., 2021).

The ZnO-NP have great industrial implications, especially in agriculture, pharmaceutics, cosmetics, electronics, rubber and textile industries, and in electro-technology and photo-catalysis (Kołodziejczak-Radzimska & Jesionowski, 2014; Kolenčík et al., 2019; Kolenčík et al., 2020). However, gradually increasing demand enhances their environmental input. This is potentially hazardous for human health and can have a long-term effect on the environment (Xia et al., 2008; Amde et al., 2017).

The transport and redistribution of water-soluble metals and soil solutions to electrodes (anode and cathode areas) are governed electrokinetic processes, such as electrolysis, electromigration, electrophoresis, and electroosmosis (Chang et al., 2006; Cang et al., 2011). These processes can simulate different soil potentials such as the electro-chemical effects on the stability charged metal (López-Vizcaíno et al., 2011). In soil chemistry, the electromigration is a governed direct motion of ions migrating to electrodes with the opposite charge (Cang et al., 2011), while the electrophoresis covers a charged colloid micelle motion in a soil-liquid medium (Chang et al., 2006). Since the electrolytic water decomposition at $\Delta E^0 = -1.23$ V is not considered a common thermodynamic process because it requires additional energy from external electrical sources (Hamid et al., 2017), electroosmosis is the flow of aqueous solutions (mostly water) from anode to cathode through connected soil pore spaces (Acar & Alshawabkeh, 1993).

Silicate sands occur naturally in soil, and their sediments accommodate limited metal sorption of ionic metal species and corresponding counterparts of bigger size fractions. A sand fraction of 0.6–1.2 mm has suitable pore size to demonstrate higher hydraulic connectivity.

DC generates alkaline pH in the cathode area, and acidic pH at anode area (Puppala et al., 1997). It supports a migration and the geochemical transformations of elements, which include:

1. metal dissolution;
2. H_2 and O_2 gas evolution on the electrodes;
3. precipitation and electro-deposition on the cathode from OH^- redundancy (Alvarez & Salinas, 2004; Vasilakopoulos et al., 2009);
4. processes related to mass and charge transfer (Acar & Alshawabkeh, 1993).

While DC effects on NP are generally recognised, information on AC application with different voltages, and low-frequency wave propagation in combination with NP is scarce. This inspired us to compare the effects of 3-hour long exposure of sand as a model porous medium under AC and DC electric fields with different voltages of 1 and 3 volts on ZnO-NP stability and mobility. We hypothesized, that such procedure will affect:

1. spatial redistribution of zinc,
2. acid-base balance near electrode surfaces,
3. structural transformation of ZnO-NP.

2   Material and methods

2.1 Pre-treatment of zinc-oxide nanoparticles

ZnO-NP with ≤40 nm average particle size (Sigma-Aldrich, Product No. 721077; Saint-Louis, Missouri, USA) were used for the evaluation of electrokinetic processes occurring under AD/DC. All ZnO-NP suspensions were diluted with deionized water to reach zinc concentration of 131.5 mg/l. These were further sonicated for 15 minutes before each experimental trial.

2.2 Characterisation of silicate sand media

Unpurified silicate sand with a declared 0.6–1.2 mm particle size range (Provodínské písky, Provodín, Czech Republic) was used as the porous medium for the quantification of electrokinetic processes. The silicate sand's pH, electrical conductivity, carbonate content and Zn availability in distilled water were determined following the standardized methods of Hrivňáková et al. (2011) (Table 1).

The saturated hydraulic conductivity was estimated by the falling head method in a reconstructed sample

Table 1   Selected silicate sand medium characteristics (mean ±standard deviation)

| pH	Carbonates content	Electrical conductivity of solution	Hydraulic saturated conductivity ($n = 8$)	Particle size distribution ($n = 3$)		Content of zinc Zn H_2O
	(%)	(mS/cm)	(cm/s)	(mm)	(%)	(mg/l)
7.71 ±0.11	0.10 ±0.01	0.08 ±0.01	0.114 ±0.008	<0.002 0.002–0.06 0.06–2 >2	0.47 ±0.05 3.9 ±0.5 95.57 ±2.5 0.07 ±n. a.	0.33 ±0.18

of total volume 100 cm^3 and air-dried bulk density of 1.72 g/cm^3 (Toková et al., 2020). The particle size distribution above 2 mm was determined by sieving, and below 2 mm by laser diffraction analysis (Igaz et al., 2020). An untreated silica sand sample was directly analysed by the wet dispersion unit of Analysette 22 laser analyser (MicroTec plus; Fritsch, Germany). Table 1 shows the percentage representation of different particle size fractions calculated by Mie the theory using following parameter values: refraction index of 1.52, absorption index of the dispersed phase was set to 0.1 and refraction index of water water was set to 1.33 (Makó et al., 2019).

2.3 Experimental design

The experiments were performed with DC and AC system using voltages of 1 V ±0.05 V or 3 V ±0.05 V. The DC experiments applied voltages of DC 1 V+ or DC3 V+ corresponding to cathode areas and anode areas.

In case of AC, AC 1 V or AC 3 V was used for Electrode 1 (E1) areas and AC 1 V or AC 3 V for Electrode 2 (E2) areas. Sinusoidal waves at 1 kHz frequency were used for both AC electric fields. The real value of 1.4 V and 4.2 V were used for sinusoidal amplitudes at 1 Vrms or 3 Vrms, respectively. The experimental control comprised a similar system without electric fields effects. The duration of each experiment was three hours. Each experiment was conducted in triplicate. For generation of DC, a power supply (Laboratory Power Supply, PS302A, 0–30 V/0.01–2 A) was used. AC was generated using a generator RIGOL, DG4162. The voltages and frequencies were periodically controlled by a M9803 true RMS MULTIMETER and the UNI-T and UTD 2025C oscilloscope (2025C, 25 MHz and 250 MS/s).

A polystyrene vessel with dimensions of 18 × 11 × 7 cm (height × width × depth) and volume of 1.3 litre was used as a type of an electro-chemical reactor to quantify the electrokinetic processes. It was filled with 1 kg of silicate sands and 320 ml of dispersed ZnO-NP solution with zinc concentration of 131.5 mg/l prior each experiment. Figure 1 depicts the most suitable laboratory setting facing graphite electrodes (with purity of 99.9%)
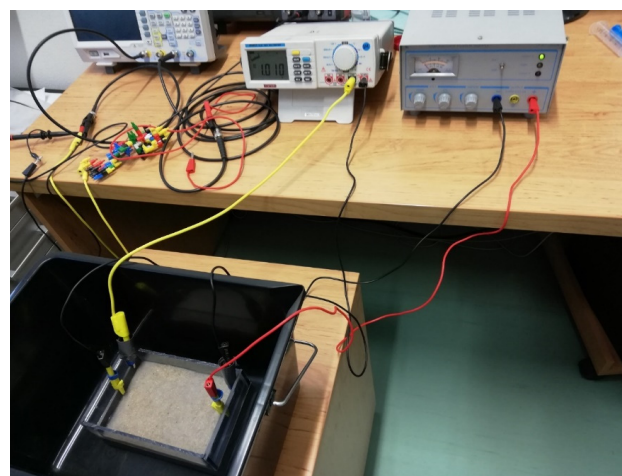
Figure 1   Experimental setup with connected DC laboratory electrical power supply, cables, graphite electrodes and multi-meter for voltage verification

(Cameselle & Gouveia, 2019). Three-dimensional size of graphite electrodes in our experiment corresponded to 100 × 50 × 3 mm.

The electrokinetic processes were quantified as the space-segment system for selected cathode-to-anode areas in DC electrical field, and Electrode 1 and 2 areas in AC electrical field shown in Figure 1, and Figure 2a, respectively.

2.4 Quantification of electrokinetic processes with ZnO-NP solution in sand media

The procedure of electrokinetic processes quantification is shown in Figure 2. The spatial intervals between the points of uniform network and electrodes were used for evaluation of the spatial equipotential patterns of DC and AC electric fields voltage uniformity in sand media with ZnO-NP. The observed equipotential patterns of AC/DC electrical voltages were later plotted in diagrams.

For determination of migrating zinc species, a flame atomic absorption spectrometer (F-AAS; Perkin Elmer 1100, USA; wavelength 213.9 nm, with deuterium background correction) was used. The calibration standard was prepared from 1,000 mg/l zinc solution
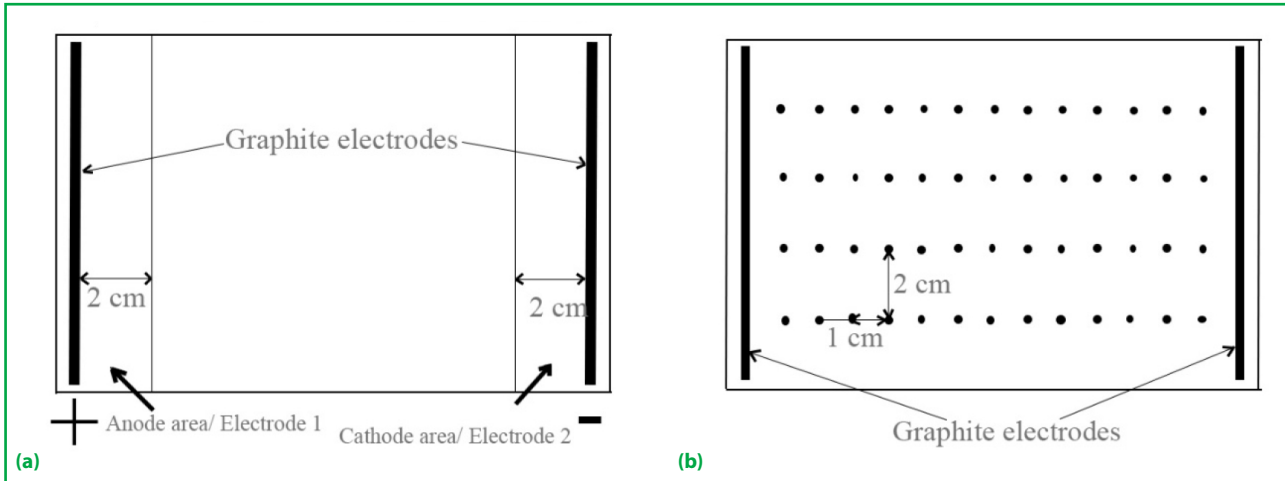
Figure 2 The schematic model of experiments with applied AC/DC electric fields (a), and the analysed points in the space between the flat graphite electrodes providing a uniform network used to determine AC/DC maps of equipotential-voltages distribution (b)

(Merck Certipur, Germany). Detection of electro-active substances was measured as sample conductivity for all determined anode-cathode, and Electrode 1 and 2 segments by HORIBA (Nanopartica SZ-100). Acid-base equilibrium changes were monitored by pH meter (WTW Lab-pH Meter inoLab pH 7110). Bruker D8 DISCOVER X-ray diffractometer was used to analyse the ZnO-NP structural symmetry transformation (Bruker, MA, USA). A 12 kW, 40 kV, 300 mA Cu-anode was used for X-ray diffractometry measurements, and unit cell parameters were calculated in TOPAS 3.0 software (Bruker, MA, USA). Some other properties of ZnO-NP have been already published elsewhere (Kolenčík et al., 2019).

3 Results and discussion

3.1 Spatial distribution of 1 V and 3 V equipotential-voltage in sand media with ZnO-NP solution under electric fields

Each type of environment in the electric field portrays the different equipotential pattern, which depends on electric field strength, environment composition and its conductivity, resistance (impedance), and the applied voltage (Portela, 1999; Chang et al., 2006; López-Vizcaíno et al., 2011). Figure 3 shows that by applying a 1 V and 3 V DC voltage to the sand media with ZnO-NP, the equipotential pattern differentiated into heterogenous
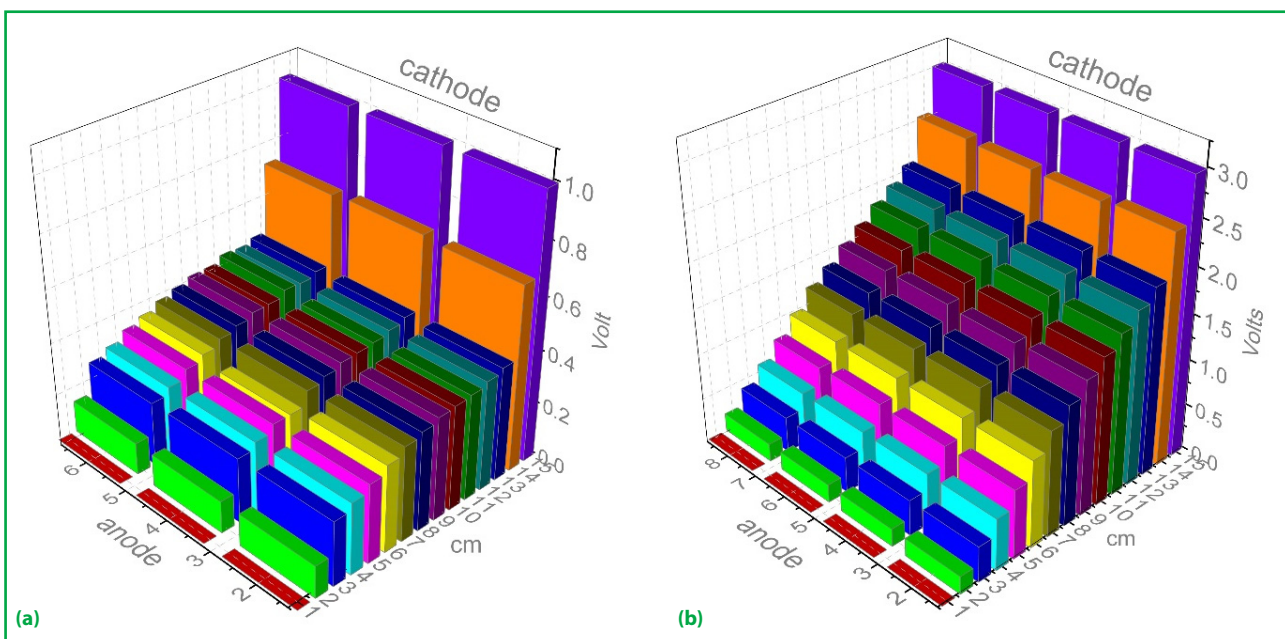
Figure 3 The equipotential pattern of sand media DC electrical field measured from anode (left) to cathode area (right) under 1 V (a) and 3 V (b) voltages
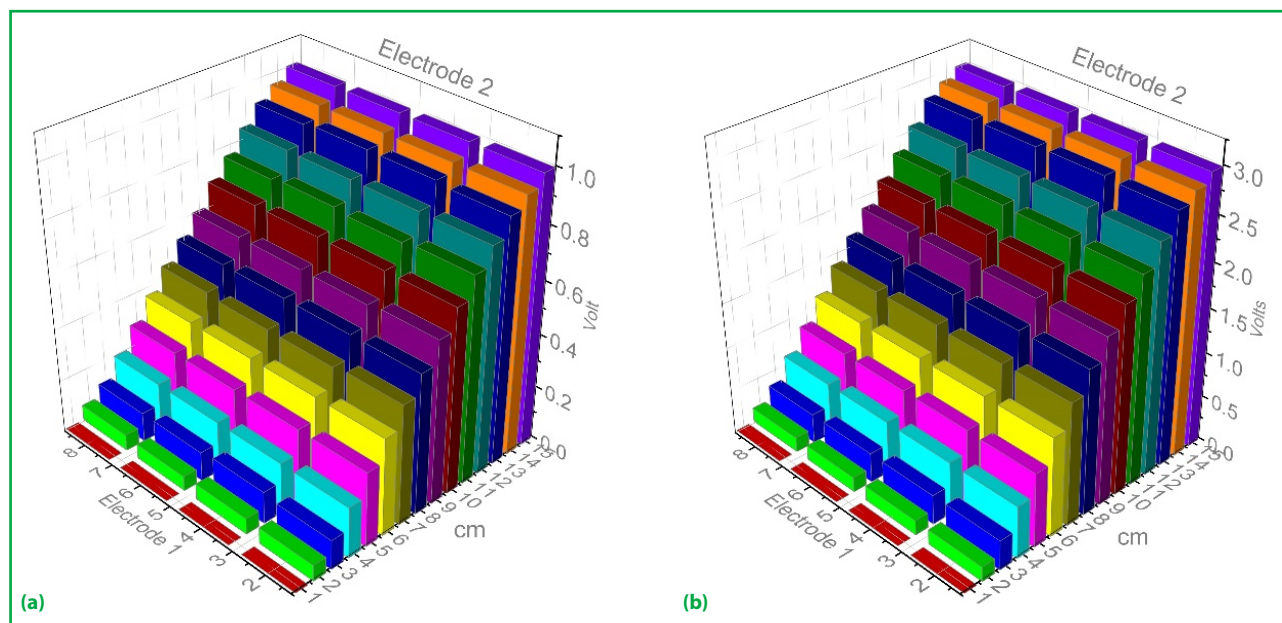
Figure 4   The equipotential pattern of sand media AC electrical field from Electrode 1 area (left) to Electrode 2 area (right) at frequency of 1 kHz under 1 V (a) and 3 V (b) voltages

voltage regions. The lower environmental polarisation effect could be caused by the relationship between our applied low voltage level and the corresponding electric currents. The electrical resistance (conduction) depends on the particle size distribution, especially the clay mineral content (Lageman, 1993), concentration of ions, and other characteristics of the environmental matrix, which influences the environmental electrical permittivity (Chang et al., 2006).

On the other hand, under applied 1 V and 3 V of AC at 1 kHz with sinusoidal waves, the equipotential pattern had a tendency to differ into almost uniform regions of voltages (Figure 4). This could be attributed to applied frequency, since this type belongs to the frequency-dependent environmental matrix (Portela, 1999; Alipio et al., 2012). Similar trends of equipotential patterns of sand media were measured either for DC or AC from opposite side of graphite electrodes (data not shown).

3.2 Effect of applied DC and AC electrical fields on pH changes of the sand media and ZnO-NP

Figure 5 shows that after three hours of treatment, the pH values at the anode were lower than at the cathode for applied 1 V and 3 voltages of DC. The pH at DC 1 V was 7.45 ±0.01 at the anode and 7.70 ±0.11 at the cathode; and pH at DC 3 V was 7.40 ±0.02 at the anode and 7.69 ±0.02 at the cathode. Although the gradually increasing acidity of the environment at the anode and increasing alkalinity at the cathode area is generally accepted process (Acar & Alshawabkeh, 1993), it remains a matter of contention how rapidly and intensively these changes and associated electrokinetic processes

occur. Water electrolysis increases ions concentration in solution in the operating electrical fields (Hamid et al., 2017) as the protons and hydroxyl ions are generated within the anodic and cathodic wells, respectively. López-Vizcaíno et al. (2011) reported that this resulted in a significant pH decrease at the anode until steady state of pH 2 was reached after 2 hours at constant voltage of 0.5 to 2 V/cm. In our experimental treatment was applied approximately 0.2 V/cm corresponding with 3 V and due to these no significant differences were observed in the case of the pH value.

The differences in our results to those of other authors were most likely due to the following; (i) the amount and chemistry of ambient ions they used differed from the ZnO-NP which required a large external energy-source to deform the double layer and caused disintegration; (ii) different experimental conditions; herein we utilised a relatively stable coarse silicate sand medium. In addition, our observations on pH changes concur with general trends without significant pH difference between anode and cathode due to treatment duration. Our 3-hour-long treatment was mostly affected by the initial experiment stages without reaching steady-state, while Lageman's (1993) trials lasted 10 hours a day and continued for 43 days with decreasing of pH 3–4 value; (iii) there is also different nanoparticle colloidal size distribution to consider. For example, Lageman (1993) electro-migrated 25–33% ionic-zinc and this depended on soil profile concentration and depth. While all those causes are relevant, the most likely difference between results is due to the longer treatment time, and total amount of ambient ions which intensified the electrical and electro-
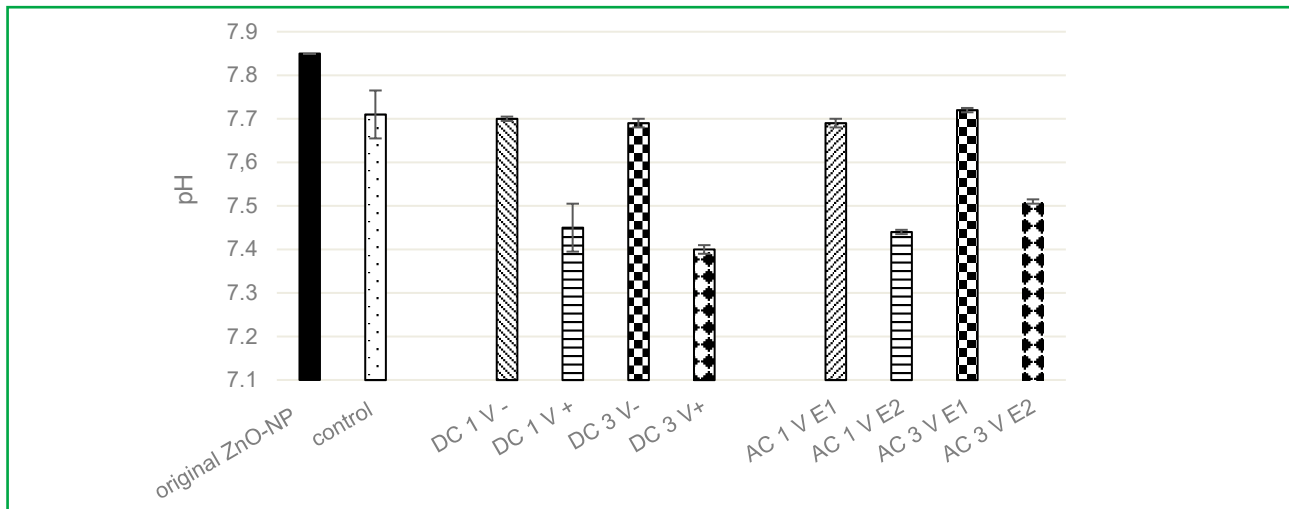
Figure 5 The changes in pH under constant low-voltage DC and AC electrical fields in sand media with ZnO-NP after three-hour-long treatment

thermal chemical gradient. This enhanced the significant pH difference observed by other researchers (Acar & Alshawabkeh, 1993; Lageman, 1993).

Moreover, no significant pH difference was observed in our experimental AC electric fields at 1 kHz, 1 V and 3 V. The Electrode 2 region had lower pH at both used voltages than Electrode 1. At Electrode 2 at 1 kHz, 1 V AC, the observed pH was 7.44 ±0.01 in comparison to pH 7.69 ±0.02 at Electrode 1. Application of 3 V led to final pH of 7.51 ±0.01 at Electrode 2 and 7.72 ±0.01 at Electrode 1 (Figure 5).

In addition, the slightly different pH of 7.71 ±0.11 in control was maintained in the three-hour-long treatment, in comparison with the pH at anode of DC treatment, and Electrode 1 areas (for both AC treatments). This was most likely time-related in the AC trials as electro-osmosis flow was generated from both electrodes simultaneously

(López-Vizcaíno et al., 2011). Finally, our pH change patterns and final values are supported by the study of Chirakkara et al. (2015).

3.3 The redistribution and potential transformation of zinc from ZnO-NP and migration of electro-active components under electrical fields

The total zinc content in the system was 131.5 mg/l and the observed zinc absorption to sand counterparts was 44.9 mg/l (34.2%). The remaining zinc content of 86.5 ±4.9 mg/l (65.8%) is considered to be associated with "free parts in the system" (Figure 6).

In addition, the original ZnO-NP sand media of colloidal solution registered 0.083 ±0.01 mS/cm electrical conductivity (Figure 7).

Ionic strength is reflected in the electrical conductance range and this qualitatively reflects charged, and
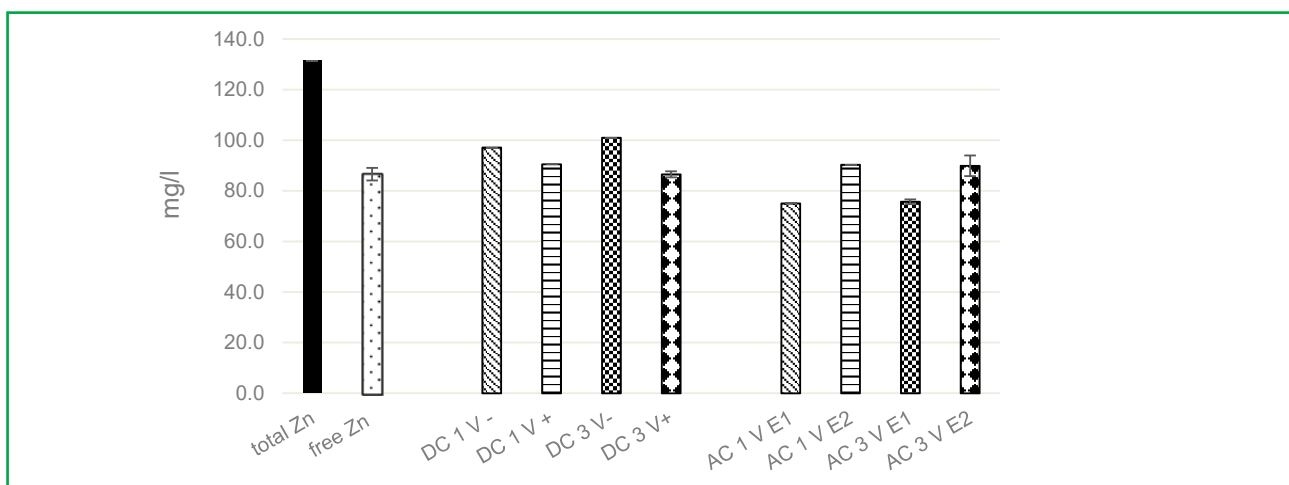
Figure 6 Analysis of DC anode-to-cathode zinc concentrations and the AC Electrode 1 and 2 regions for both voltages. The three-hour-long ZnO-NP treatment in sand media was conducted with constant low-level DC and AC electrical fields
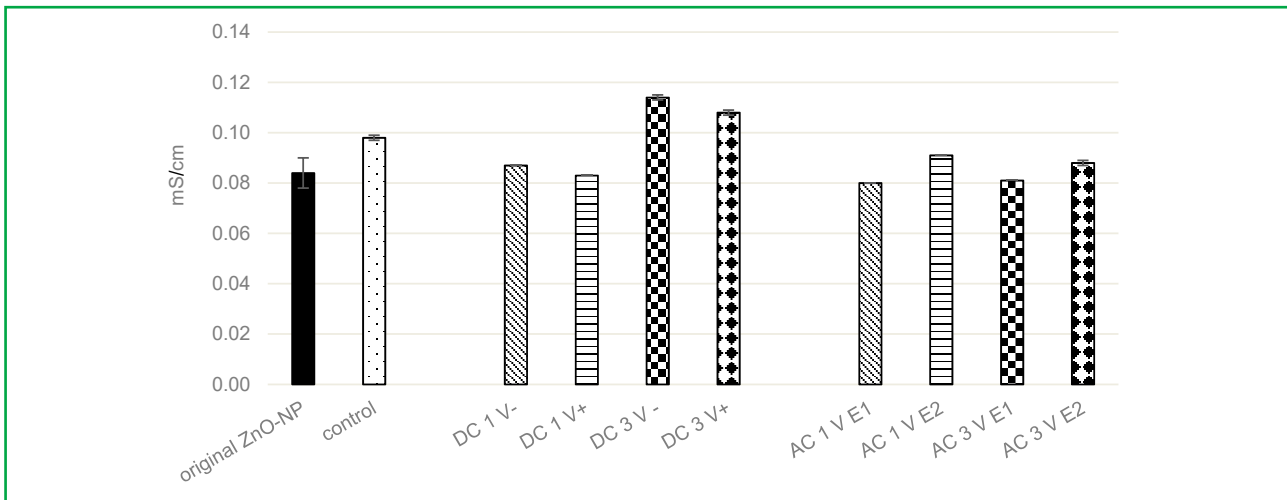
Figure 7 Analysis of the electrical conductivity of ZnO-NP colloidal solution at DC electrical field anode-to-cathode areas, and AC electrical field strengths at the Electrode 1 and 2 regions after three-hour-treatment compared to controls

un-charged ions in solution. This entire system then acts as one electrochemical cell (López-Vizcaíno et al., 2011). Therefore, our ZnO-NP solutions with associated free ions could have slightly restricted or unlimited motion from the relatively high hydraulic-guaranteed coarse silicate sand pore size (Table 1). This provides appropriate conditions for relatively long-term nanoparticle colloidal stability with Van der Walls attraction and repulsion forces, or ambient-ion free migration. There was no literature found for nanoparticle behaviour under electrical field influence in this type of media.

Additional differences in constant DC voltages at the anode and cathode and electric conductivities for zinc concentration are; 1 V anode area 90.50 ±0.01 mg/l and at the cathode 97.10 ±0.01 mg/l – 5.01%; 3 V at anode area 86.50 ±2.40 mg/l and 101.0 ±0.01 mg/l – 11.02% at the cathode; electrical conductivity was greater at the cathode than at the anode. Meanwhile, the control registered 86.55 ±4.95 zinc content and 0.08 ±0.01 mS/cm electrical conductivity, with relatively uniform ionic strength throughout the entire system.

These results differ slightly to those reported by López-Vizcaíno et al. (2011). Their anode-to-cathode electrical conductivity provided a flat profile at 2, 4 and 6 hour-treatments. The DC zinc and other ambient ion anode-to-cathode and control concentration ranges were confirmed, and the differences were most likely due to the for short 3-hour experimental treatment and the relatively homogenous ZnO-NP solution without others electro-active compounds.

In addition, Lageman (1993) recorded that the application of more intense DC electrical fields resulted in higher zinc content and more electroactive compounds at the cathode than at the anode. Therefore, we only

speculate that the electro-migration of zinc-ionic and ionic species corresponds to electrophoresis-enhanced corresponding to charged ZnO-NP (Chang et al., 2006). This is most likely detection of diffusion or other electro-controlled motion to Helmholtz' double layer distance from the cathode surface (Iyer, 2001). This conforms to applied electrical potential voltages, electro-thermal gradient, pH and other physical-chemical components which govern zinc and ambient ion electro-migration in DC electrical fields (Lageman, 1993; Cameselle & Gouveia, 2019).

Figure 6 illustrates the following difference in zinc concentration between the electrodes in AC 1 kHz, 1 V and 3 V in constant electrical fields; 1 Volt was 75.00 ±0.01 mg/l at Electrode 1 and 90.30 ±0.01 mg/l at
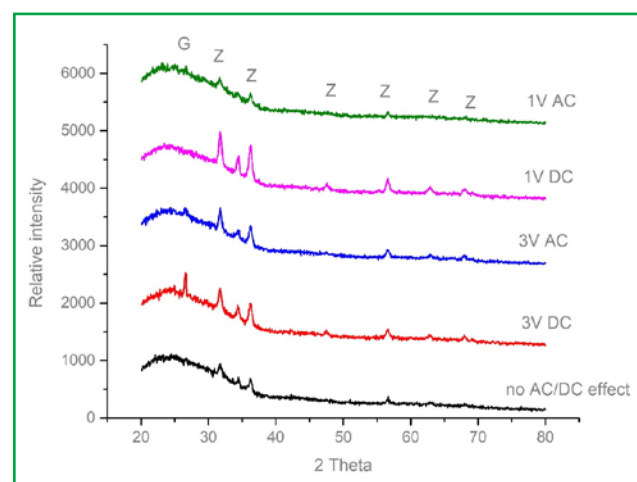
Figure 8 X-ray diffraction analysis of zinc oxide nanoparticles (Z), and graphite (G) under 1 V, and 3 V DC and AC after the experimental three-hour-long treatment. The control with ZnO-NP was not subjected to the electric fields

Electrode 2 and 11.63%; 3 Volts was at Electrode 1 area (75.65 ±1.85 mg/l at Electrode 1 and 89.85 ±8.15 mg/l at Electrode 2 and 10.79%).

Figure 7 then highlights the significant difference in electrical conductivity; the Electrode 2 areas for both 1 kHz 1 V and 3 V possess higher ionic strength than the Electrode 1 regions. In addition, slight differences in zinc concentration were observed in DC electrical field effect compared to both AC and the control.

It is also interesting that the higher analysed Zn for both voltage treatments at Electrode 2 has only weak tendency, because this contrasts with accepted knowledge. In our case alternating current does not provide uniform side-accumulation of heavy metals in this hydraulic-guaranteed saturated coarse sand pore medium.

Moreover, Electrode 1 and 2 regional differences of 11.63% for applied AC 1 V and 10.79% for 3 V do not confirm the expected correlation between little bit enhanced electric fields and zinc-related electro-migration ability. This most likely resulted from our applied low-level frequency at 1 kHz, and this is similar to the noted zinc differences. It is evident that the different parameters in this soil-type are frequency-dependent (Alipio et al., 2012). The applied 1 kHz frequency could cause slight destruction to nanoparticle crystal symmetry with accompanying Helmholtz double layer, and zeta potential.

Although the Zn concentration from selected areas and electrical conductivity point to slight differences in the results, however there was no significant distinction in crystal symmetry, size distribution or accompanying properties (Figure 8). This is most likely because of relationships with partial electro-deposition or electro-regulated zinc crystallisation at the solution and electrode interface (Alvarez & Salinas, 2004). Research in this area includes the nucleation and growth of new crystalline Zn phases or 2D layers on the electrode surface with low-carbon steel (Vasilakopoulos et al., 2009); employment of carbon electrodes (Torrent-Burgués & Guaus, 2007) and highly oriented pyrolytic graphite (Alvarez & Salinas, 2004). These studies, however, have electrolyte solution pH below 5 and a large number of organic and inorganic components. Moreover, some other studies reported pH slightly over 7 for all experiments with ZnO-NP solutions. This also applies to ambient ions. For example, carbonates around 0.10% normally correspond to ions with buffer capacity, but they do not provide the expected increase in ionic solution strength or ion-governed crystallisation processes. We also noted electrode deterioration in our 3 V experiments with DC and AC electrical field application, but this damage further identifies the relative strength of these electric fields.

4 Conclusions

The electrokinetic reaction experiments were performed using the zinc oxide nanoparticle solution and silicate sand pore-media with high hydraulic conductivity. This was subjected to three-hour-long exposure to 1 V and 3 V direct current (DC) and 1 kHz 1 V and 3 V alternating currents (AC) with sinusoidal waves. The observations provided the following results:

❍ There were no uniform equipotential lines in the voltage-independent silicate sands-pore media subjected to 1 V and 3 V DC. In contrast, the lines were quite apparent in the spatial distribution of the applied 1 kHz 1 V and 3 V AC electrical fields.

❍ The pH was slightly lower at the anode than at the cathode for both DC 1 V and 3 V exposure after three hours. Similar trends were also apparent in the 1 kHz 1 V and 3 V AC electric fields treatments. There was slightly lower pH at Electrode 2 than at Electrode 1, and the initial stages of the electrokinetic process caused pH to range from 7.40 to 7.82 for all experimental systems when compared to control pH = 7.71 ±0.11.

❍ Higher Zn concentrations were observed at the cathode in comparison with the anode region. The differences were approximately 5% for 1 V DC exposure and 11% for 3 V DC, respectively. These results conform to the related pH and electrical conductance determinations of greater magnitude at the cathode in comparison with the anode. Analysis also showed higher Zn content at Electrode 2 than at Electrode 1 for the 1 kHz 1 V and 3 V AC electric fields. These results support the established higher electrical conductance at Electrode 2, but they do not correlate with the slightly lower Electrode 2 pH values.

❍ In conclusion, although the expected structural transformation of zinc oxide nanoparticles as agrochemical was not confirmed under the influence of 1 V, and 3 V DC and 1 V, and 3 V AC electrical fields, the deterioration in the chemically and physically resistant graphite electrodes was observed.

References

Acar, Y.B., & Alshawabkeh, A.N. (1993). Principles of electrokinetic remediation. *Environmental Science & Technology*, 27(13), 2638–2647.
https://doi.org/10.1021/es00049a002

Alipio, R.S. et al. (2012). Electric fields of grounding electrodes with frequency dependent soil parameters. *Electric Power Systems Research*, 83(1), 220–226.
https://doi.org/10.1016/j.epsr.2011.11.011

Alvarez, A.E., & Salinas, D.R. (2004). Nucleation and growth of Zn on HOPG in the presence of gelatine as additive. *Journal of Electroanalytical Chemistry*, 566(2), 393–400.
https://doi.org/10.1016/j.jelechem.2003.11.051

Amde, M. et al. (2017). Transformation and bioavailability of metal oxide nanoparticles in aquatic and terrestrial environments. A review. *Environmental Pollution*, 230, 250–267.
https://doi.org/10.1016/j.envpol.2017.06.064

Cameselle, C., & Gouveia, S. (2019). Phytoremediation of mixed contaminated soil enhanced with electric current. *Journal of Hazardous Materials*, 361, 95–102.
https://doi.org/10.1016/j.jhazmat.2018.08.062

Cang, L. et al. (2011). Effects of electrokinetic-assisted phytoremediation of a multiple-metal contaminated soil on soil metal bioavailability and uptake by Indian mustard. *Separation and Purification Technology*, 79(2), 246–253.
https://doi.org/10.1016/j.seppur.2011.02.016

Hamid, S.B.A. et al. (2017). Photocatalytic water oxidation on ZnO: a review. *Catalysts*, 7(3),93, 1–14.
https://doi.org/10.3390/catal7030093

Hrivňáková, K. et al. (2011). *The uniform methods of soil analysis*. VÚPOP, Bratislava (136 p.).

Chang, J.-H. et al. (2006). Remediation and stimulation of selected chlorinated organic solvents in unsaturated soil by a specific enhanced electrokinetics. *Colloids and Surfaces A: Physicochemical and Engineering Aspects*, 287(1), 86–93.
https://doi.org/10.1016/j.colsurfa.2006.03.039

Chirakkara, R.A. et al. (2015). Electrokinetic amendment in phytoremediation of mixed contaminated soil. *Electrochimica Acta*, 181, 179–191.
https://doi.org/10.1016/j.electacta.2015.01.025

Igaz, D. et al. (2020). Laser diffraction as an innovative alternative to standard pipette method for determination of soil texture classes in Central Europe. *Water*, 12(5), 1232. 1–16.
https://doi.org/10.3390/w12051232

Iyer, R. (2001). Electrokinetic remediation. *Particulate Science and Technology*, 19(3), 219–228.
https://doi.org/10.1080/02726350290057813

Kolenčík, M. et al. (2019). Effect of foliar spray application of zinc oxide nanoparticles on quantitative, nutritional, and physiological parameters of foxtail millet (*Setaria italica* L.) under field conditions. *Nanomaterials*, 9(11), 1559, 1–11.
https://doi.org/10.3390/nano9111559

Kolenčík, M. et al. (2020). Foliar application of low concentrations of titanium dioxide and zinc oxide nanoparticles to the common sunflower under field conditions. *Nanomaterials*, 10(8), 1619, 1–20.
https://doi.org/10.3390/nano10081619

Kolenčík, M. et al. (2021). Effect of TiO_2 as plant-growth stimulating nanomaterial on crop production. In Singh, V.P.et al. (Eds.) *Plant Responses to Nanomaterials, Recent Interventions, and Physiological and Biochemical Responses*. (1st ed.). Cham, Switzerland: Springer Nature Switzerland AG (pp. 129–144).

Kołodziejczak-Radzimska, A., & Jesionowski, T. (2014). Zinc oxide-from synthesis to application: A review. *Materials*, 7(4), 2833–2881. https://doi.org/10.3390/ma7042833

Lageman, R. (1993). Electroreclamation. Applications in the Netherlands. *Environmental science & Technology*, 27(13), 2648–2650. https://doi.org/10.1021/es00049a003

López-Vizcaíno, R. et al. (2011). Electro-osmotic fluxes in multi-well electro-remediation processes. *Journal of Environmental Science and Health – Part A Toxic/Hazardous Substances and Environmental Engineering*, 46(13), 1549–1557.
https://doi.org/10.1080/10934529.2011.609458

Makó, A. et al. (2019). Evaluation of soil texture determination using soil fraction data resulting from laser diffraction method. *International Agrophysics*, 33, 445–454.
https://doi.org/10.31545/intagr/113347

Portela, C. (1999). Measurement and modeling of soil electromagnetic behavior. In *1999 IEEE International Symposium on Electromagnetic Compatability. Symposium Record* (Cat. no. 99CH36261) 2, 1004–1009.
https://doi.org/10.1109/ISEMC.1999.810203

Puppala, S.K. et al. (1997). Enhanced electrokinetic remediation of high sorption capacity soil. *Journal of Hazardous Materials*, 55(1), 203–220.
https://doi.org/10.1016/S0304-3894(97)00011-3

Rudd, A.L., & Breslin, C.B. (2000). Photo-induced dissolution of zinc in alkaline solutions. *Electrochimica Acta*, 45(10), 1571–1579. https://doi.org/10.1016/S0013-4686(99)00322-9

Sturiková, H. et al. (2018). Zinc, zinc nanoparticles and plants. *Journal of Hazardous Materials*, 349, 101–110.
https://doi.org/10.1016/j.jhazmat.2018.01.040

Toková, L. et al. (2020). Effect of biochar application and re-application on soil bulk density, porosity, saturated hydraulic conductivity, water content and soil water availability in a silty loam Haplic Luvisol. *Agronomy*, 10(7), 1005, 1–17.
https://doi.org/10.3390/agronomy10071005

Torrent-Burgués, J., & Guaus, E. (2007). Effect of tartaric acid in the electrodeposition of zinc. *Journal of Applied Electrochemistry*, 37(5), 643–651.
https://doi.org/10.1007/s10800-007-9296-2

Vasilakopoulos, D. et al. (2009). Electrocrystallisation of zinc from acidic sulphate baths; A nucleation and crystal growth process. *Electrochimica Acta*, 54(9), 2509–2514.
https://doi.org/10.1016/j.electacta.2008.11.059

Xia, T. et al. (2008). Comparison of the mechanism of toxicity of zinc oxide and cerium oxide nanoparticles based on dissolution and oxidative stress properties. *ACS nano*, 2(10), 2121–2134. https://doi.org/10.1021/nn800511k